ChemSusChem

Research Article
doi.org/10.1002/cssc.202200840

Chemistry Europe
European Chemical Societies Publishing

www.chemsuschem.org

Hydrazine Energy Storage: Displacing N_2H_4 from the Metal Coordination Sphere

Andrew J. McNeece[+],[a] Adam Jaroš[+],[b] Enrique R. Batista,*[b] Ping Yang,*[c] Brian L. Scott,[a] and Benjamin L. Davis*[a]

Hydrogen carriers, such as hydrazine (N_2H_4), may facilitate long duration energy storage, a vital component for resilient grids by enabling more renewable energy generation. Lanthanide coordination chemistry with N_2H_4 as well as efforts to displace N_2H_4 from the metal coordination sphere to develop an efficient catalytic production cycle were detailed. Modeling the equilibrium of different ligand coordination, it was predicted that strong sigma donor molecules would be required to displace N_2H_4. Monitoring competition experiments with nuclear magnetic resonance confirmed that trimethyl phosphine oxide, dimethylformamide, and dimethyl sulfoxide displaced N_2H_4 in large or small lanthanide complexes.

Introduction

In 2020 the United States Department of Energy (USDOE) set forth a Grand Challenge focused on Energy Storage, the first comprehensive approach by that agency.[1] Given the success of lithium-ion battery technology to address short energy storage durations (<4 h),[2] the focus of storage research has shifted to long duration approaches, which favour technologies where power and energy are decoupled to enable flexible grid installations. Liquid hydrogen carriers represent one method that can leverage existing infrastructure and utilize the high efficiency/maturity of proton exchange membrane (PEM) fuel cells to release the stored energy when needed.[3] Toward that end we are focusing on hydrazine (N_2H_4), which has 12.5% H_2 by weight and has been incorporated into fuel cell applications.[4,5] Although made industrially by several processes, N_2H_4 is generally made by the oxidation of NH_3 whose current infrastructural and carbon footprint are substantial.[6] If N_2H_4 could be formed directly from dinitrogen (N_2), in a potentially decentralized fashion, then energy grids could be safer while allowing for greater renewable energy generation.

There are many examples in the literature where N_2H_4 can be formed from N_2, with molecular transition metal catalysts recently reviewed[7] and a multitude of materials studies.[4,5] Seminal studies by Shilov[8] and Bercaw[9] showed that low-valent group IV metal complexes are capable of reductively binding N_2 and, upon treatment with a strong acid (protolytic conditions; e.g., HCl), could be transformed to $N_2H_4 \cdot 2HCl$. Myriad examples of new metal complexes followed containing diverse transition metals such as Fe,[10–12] Cr,[13] Mo,[10] and Ru.[14] There have also been electrocatalytic examples, in particular a trinuclear nickel complex,[15] which is surprising given the thermodynamic preference for NH_3 formation.[16] A common challenge for most transition metal systems is the concurrent formation of ammonia (NH_3) with N_2H_4 and formation of N_2H_4 salts. Methods do exist for removal of NH_3, which is a fuel cell poison,[17] but ideally a process that can generate N_2H_4 without NH_3 contamination or N_2H_4 salts represents a more efficient process overall.

Innovative coordination studies in the 1990s and more recent N_2 reduction work by Evans[18–20] suggest that a pathway to atom-efficient formation of N_2H_4 is possible. N_2H_4 can form stable samarium complexes with the first example being $(C_5Me_5)_2Sm(N_2H_4)(THF)BPh_4$.[18] Later it was demonstrated that $(N_2)^{2-}$ could be protonated to form $[(N_2H_2)^{2-}]$[21] and eventually N_2H_4, albeit with different ligand configurations.[19] The aforementioned precedents are high yielding, with no explicit NH_3 formation, suggesting N_2 may be transformed to N_2H_4 selectively. Recent work by Xi and co-workers elegantly shows that a single ligand system is able to make functionalized hydrazines, lending additional support to the idea of making N_2H_4. In the latter case strong alkylating agents were required to generate the hydrazines and form Ln–halide bonds.[22]

Given the literature precedent for transforming N_2 to N_2R_4 (R=H or alkyl), we wished to explore releasing N_2R_4 from the coordination sphere of the metal complex without strong acids. The latter results in procatalysts with halide ligands, which

[a] A. J. McNeece,[+] B. L. Scott, B. L. Davis
MS K763, MPA-11 Materials Synthesis and Integrated Devices
Los Alamos National Laboratory
Los Alamos, New Mexico, 87545 (USA)
E-mail: bldavis@lanl.gov
[b] A. Jaroš,[+] E. R. Batista
MS B258, T-CNLS Center for Nonlinear Studies
Los Alamos National Laboratory
Los Alamos, New Mexico, 87545 (USA)
E-mail: erb@lanl.gov
[c] P. Yang
MS B221, T-1 Physics and Chemistry of Materials
Los Alamos National Laboratory
Los Alamos, New Mexico, 87545 (USA)
E-mail: pyang@lanl.gov
[+] These authors contributed equally to this work

Supporting information for this article is available on the WWW under https://doi.org/10.1002/cssc.202200840

require powerful reducing agents (KC_8) to remove, along with hydrazine salts.[22] Using a combined theoretical and experimental approach, we have identified ligands that are able to displace N_2H_4 from the metal coordination sphere without strong acids, such that a method for producing N_2H_4 atom efficiently may be possible.

Results and Discussion

If an energy efficient pathway to N_2H_4 is possible, avoiding strong Ln–halide bonds is desirable. To this end we sought to study the coordination chemistry of lanthanide–N_2H_4 complexes with the aim of displacing N_2H_4 more efficiently, avoiding anionic ligands altogether. Using a density functional theory (DFT) approach with known Ln–N_2H_4 complexes as a guide, we examined the equilibrium (Figure 1) with a selection of possible coordinative moieties consisting of monodentate neutral ligands (L, Figure 2), C_5Me_5 rings, and lanthanide/lanthanide-like metal ions (La^{3+}, Y^{3+}, Lu^{3+}). The ligands examined contain various types of coordinating atoms and groups (carbonyls, phosphine oxides, or sulfoxides as hard ligands, and alcohols, ethers, heterocycles, phosphine, and acetonitrile as soft ligands).

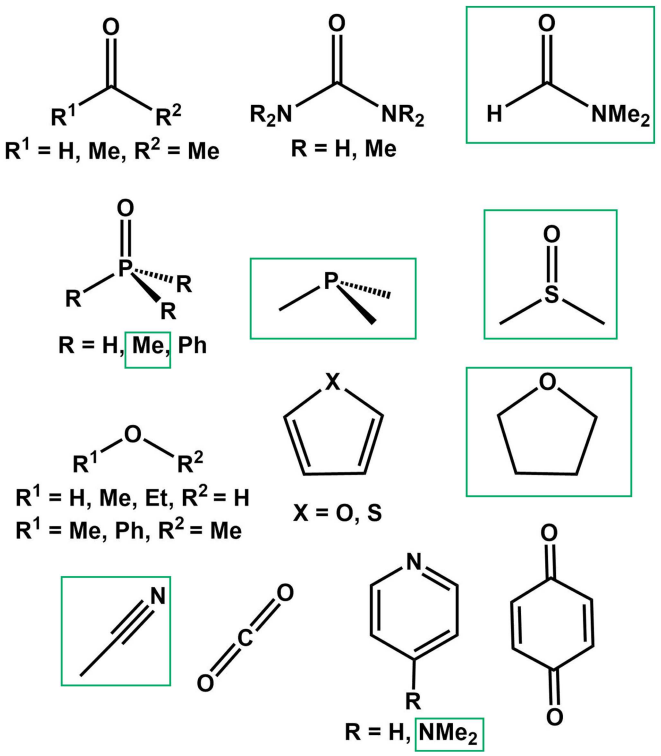

Figure 2. Ligands evaluated to displace N_2H_4 from the lanthanide coordination sphere. Experimentally tested ligands are highlighted in green.

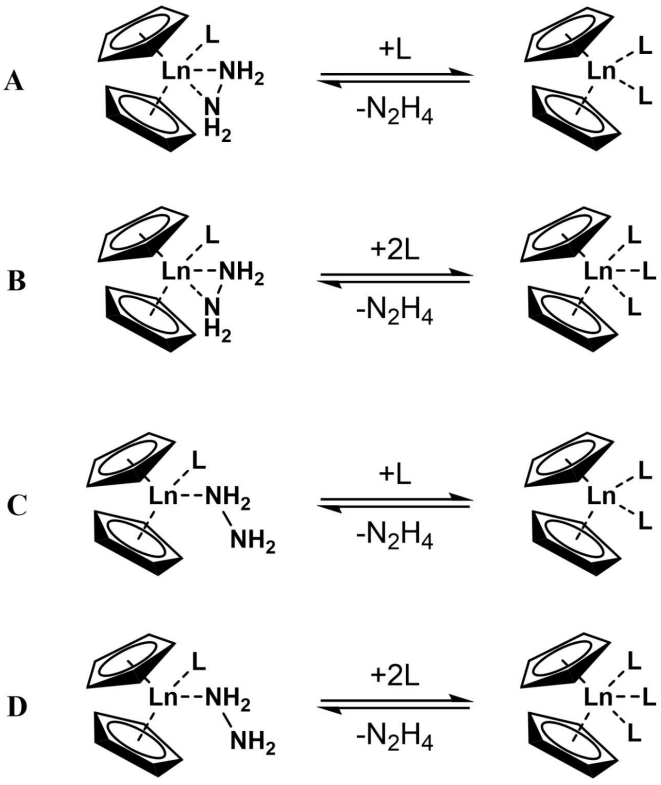

Figure 1. Equilibrium of coordinated N_2H_4 vs. variable ligand L. Both monodentate and bidentate forms of N_2H_4 were considered as well as complexes with two and three ligands. Counter anions were not modeled since we shall use noncoordinating borates. Methyl groups on the Cps were omitted for clarity.

To evaluate possible complexes that may exist in the solution, different combinations of metals and ligands, including both haptic modes for N_2H_4 (only η^2-N_2H_4 is in the CSD (Cambridge Structural Database) for Ln complexes),[23] were evaluated with two C_5Me_5 ligands to reflect known complexes and sterically balance the cationic complex (Figure 2). Calculations show (Table 1; for more extensive combinations with yttrium see Table S2) that in most of the studied cases η^2-N_2H_4 is preferred except when the ligand was Me_3PO, Ph_3PO, DMSO, and urea. Complexes containing two L and one η^1-N_2H_4 were calculated to be thermodynamically unfavorable. We attribute this to steric repulsion and the preference for bidentate binding. Complexes with three ligands were also found to be unfavorable for the same reason, with few exceptions (i.e., when combining the largest metal ion, such as La^{3+}, with ligands without significant steric demands, such as MeCN). In

Table 1. $\Delta_r G$ (kcal) of lowest energy equilibrium depicted in Fig 1 with selected ligands – negative values indicate favoured displacement. Capitalized letter indicates which reaction in Fig 1 the value refers.

Ligand↓/Metal→[1]	La	Y	Lu
$Me_3P{=}O$	−8.3 (C)	−7.6 (C)	−5.6 (C)
DMF	−6.8 (B)	−4.6 (A)	−3.8 (A)
DMSO	−5.1 (D)	−2.9 (C)	−2.7 (C)
DMAP	−1.8 (A)	1.3 (A)	1.5 (A)
MeCN	0.5 (B)	3.1 (A)	1.5 (A)
THF	2.3 (A)	6.6 (A)	7.6 (A)
PMe_3	7.0 (A)	7.9 (A)	10.8 (A)

summary, most of the studied displacement reactions proceed according to reaction A; specific cases are shown in Table 1. Reaction energies of yttrium complexes for all of the reactions depicted in Figure 1 are summarized in Table S3. Reaction energies of yttrium complexes with THF coordinated together with hydrazine as the displaced ligand are summarized in Table S4.

Calculated values of the change in free energy of the reaction ($\Delta_r G$, kcal) for the displacement reaction of THF from yttrium complexes show that Me_3PO, DMF, Ph_3PO, DMSO, and urea ligands are thermodynamically favored to bind preferentially. Comparison of the reaction energies between La^{3+} and Y^{3+} and the experimental data show that the larger metal ion, with lower Lewis acidity, is more favorable for N_2H_4 coordination (Table 1).

In general, the calculations show that the ligands capable of displacing the N_2H_4 are either organic oxides of heteroatoms (P and S) or carbonyls. Steric repulsion also plays a role, although it heavily depends on the particular ligand and its structure. Population and bonding analyses show that the displacing ligands are more negatively charged on the coordinating atom (Me_3PO −1.13 vs. THF −0.53), with respect to the incumbent ligand, and metal centers are more positively charged in the complexes with them (Me_3PO 1.94 vs. THF 1.83). Mayer bond order of the interaction between the metal ion and ligands shows stronger bonding to the L compared to the N_2H_4 in case of displacing ligands (Me_3PO, M–L 0.33, M–N_2H_4 0.15), and vice versa (THF, M–L 0.15, M–N_2H_4 0.21). When the displacing ligand is attached, the electron density is thus compensated by the ligands, effectively weakening it and favoring the displacement reaction. All studied bonding and structural parameters are summarized in the Supporting Information (Tables S5 and S6). Comparison between various phosphine–oxide ligands also shows that steric repulsion influences the displacement reaction energy: the largest Ph_3PO ligand is performing worse in the displacement. Thus, the ideal ligands for the hydrazine displacement should exhibit a strong interaction with the metal ion while also not being too sterically demanding.

To experimentally check our predictions, $(C_5Me_5)_2Ln(N_2H_4)(THF)BPh_4$ [Ln=La (**1**), Y, (**2**), Lu (**3**)] complexes were synthesized in 80–84% yield by combining N_2H_4 with the $(C_5Me_5)_2Ln(THF)_2BPh_4$ [generated from $(C_5Me_5)_2Ln(C_3H_5)$[24] and Et_3NHBPh_4]. Nuclear Overhauser effect spectroscopy (NOESY) experiments indicate coordination of N_2H_4 with a correlation peak between the Cp* and N_2H_4 resonances in complex **1** (Figure S7). In order to be confident that the complexes were of the highest purity and thus assured that the chemical shifts only represent coordinated N_2H_4, **1** and **2** were crystallized and definitively characterized by X-ray crystallography (Figure 3). Similar to the Sm analogue, La and Y asymmetrically bind N_2H_4, with La–N1 2.614(3) Å and La–N2 of 2.585(3) Å yielding a difference of 0.029 Å, and Y–N1 2.4503(18) Å and Y–N2 2.4336(17) Å with a difference of 0.017 Å. Within uncertainty, these values are reasonable and comparable to the known Sm–N_2H_4 structure (0.031 Å). The Cp*(center)–La–Cp*(center) angle is 135.3°, slightly smaller than 138.9° observed for Sm and 139.2° for yttrium, but as expected when comparing analogous

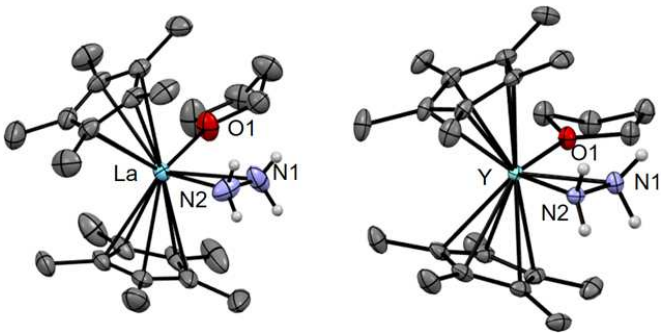

Figure 3. Crystal structure of **1** and **2** with ellipsoids drawn at the 50% probability. Non–N–H hydrogens have been omitted for clarity. Selected bond lengths and angles: La–N1 2.614(3) Å, La–N2: 2.585(3) Å, La–O1 2.548(3) Å, La–Cp*(centroid) avg: 2.55 Å, Cp*–La–Cp* 135.3°. Y–N1 2.450(18) Å, Y–N2: 2.433(17) Å, Y–O1 2.408(3) Å, Y–Cp*(centroid) avg: 2.38 Å, Cp*–Y–Cp* 139.2°.

structures across the lanthanide series. A calculated structure of Y^{3+} complex shows Y–N1 distance of 2.519, Y–N2 of 2.482, and Y–O1 of 2.443 Å, and Cp*(center)–Y–Cp*(center) angle of 140°. La^{3+} complex distances are La–N1 of 2.755, La–N2 of 2.658, and La–O1 of 2.578 Å and Cp*(center)–La–Cp*(center) angle of 140°. These values are in reasonable agreement with the crystal structures, with differences probably arising from the crystal packing as calculations were performed in the gas phase. In general, lanthanum-containing complexes have greater distances between the coordinating atoms and metal ion, as expected given the greater ionic radius of La^{3+}.

With our modelling efforts as a guide, we used nuclear magnetic resonance (NMR) spectroscopy to study N_2H_4 coordination with complexes **1**–**3** dissolved in THF-d_8 at room temperature. 2 or 10 equiv. of candidate ligands were used and the change in chemical shift was noted (Table 2). Where

Table 2. ^{1}H NMR chemical shift data for $(C_5Me_5)_2Ln(N_2H_4)(THF)BPh_4$ at 20 °C.

Metal	Ligand	δ N_2H_4 (THF-d_8) [ppm]
n/a	N_2H_4	3.0
La	N_2H_4	3.4–3.5
	Me_3PO (2 equiv.)	2.96
	DMSO (2 equiv.)	3.04
	DMF (2 equiv.)	3.02
	DMAP (2 equiv.)	3.74
	MeCN	3.32 (3.18)[a]
	PMe_3 (2 equiv.)	3.28
Y	N_2H_4	3.58
	Me_3PO (2 equiv.)	3.0
	DMSO (2 equiv.)	3.21
	DMF (2 equiv.)	3.17 (3.05)
	DMAP (2 equiv.)	3.65
	MeCN	3.48 (3.33)
	PMe_3 (2 equiv.)	3.31
Lu	N_2H_4	3.60
	Me_3PO (2 equiv.)	2.96
	DMSO (2 equiv.)	3.24

[a] Values in parentheses indicate shift with 10 equiv.

possible, a NOESY experiment was also used to gauge spatial proximity of N_2H_4 with other ligands on the complex.

The chemical shift for N_2H_4 when the best donor ligand, Me_3PO, is combined with **1**–**3**, is essentially the same as unbound N_2H_4 (≈3.0 ppm, Figures S8–S10). The aforementioned resonance is notable for being broad to different degrees in each case. This upfield shift in the resonance for N_2H_4 suggests displacement from the metal coordination sphere, confirming our model prediction. Due to the weaker intensity, we did check independent mixing of Me_3PO and N_2H_4, which showed no reaction. In case of complex **3**, ^{31}P NMR spectroscopy indicates a downfield shift of the Me_3PO resonance from 33 to 59 ppm, providing addition support that N_2H_4 has been displaced with Me_3PO (Figure S11). The distinct doublet at around 1 ppm in all reactions is characteristic of C_5Me_5—H, indicating some decomposition of the complex has occurred. Therefore, our focus shifted to more stable complex/ligand pairs.

Dimethyl sulfoxide (DMSO) and dimethylformamide (DMF) were both predicted to displace N_2H_4 in complexes **1**–**3** at room temperature with 2 equiv. added. For complex **1**, this seems to be the case by NMR spectroscopy: the N_2H_4 shift for DMSO is 3.04 ppm and for DMF 3.02 ppm, very close to the unbound resonance of 3.0 ppm (Figures S12 and S18). The displacement was confirmed with a NOESY experiment of complex **1**, which no longer showed a cross peak for the N_2H_4 and the Cp*–CH_3 (Figure S13). For the smaller lanthanides (complexes **2** and **3**), the N_2H_4 resonance is at an intermediate value between coordinated (≈3.6 ppm) and unbound (≈3.0 ppm), at 3.17–3.24 ppm (Figures S14, S17, S19). This value suggests some exchange, which is corroborated by a weak NOE between the DMSO/Cp*–CH_3 and N_2H_4/Cp*–CH_3 in complex **2** (Figures S15 and S16). In addition, when 10 equiv. of DMF is added to complex **2**, the N_2H_4 shift moved further upfield to 3.05 ppm, very close to unbound N_2H_4 (Figure S19).

N,*N*′-dimethylaminopyridine (DMAP) formally is predicted to have sufficient thermodynamic power to displace N_2H_4 in complex **1**, with $\Delta_rG = -1.8$ kcal (Table 1). When DMAP is combined with complex **1**, the chemical shift for N_2H_4 is 3.74 ppm, further downfield-shifted from the coordinated N_2H_4 at 3.4–3.5 ppm (Figure S20). Based on the observations for DMSO/DMF, whose predicted coordination free energies are more negative than DMAP, empirically the lack of displaced N_2H_4 is not surprising. NOESY experiments support this assertion, with evident cross peaks between N_2H_4 and the Cp* methyl resonances, in addition to cross peaks for N_2H_4 and DMAP(ortho) protons (Figure S21). Complex **2** behaved in a similar fashion with DMAP. At this time, we cannot rationalize the downfield shift of N_2H_4 in this complex.

A nitrile coordinate group was also examined, with acetonitrile (MeCN) being a readily accessible example. Modelling the displacement of N_2H_4 with MeCN favored the formation of three MeCN coordinated in the case of the largest lanthanide, $(C_5Me_5)_2La(MeCN)_3^+$, and two for smaller relatives, $(C_5Me_5)_2Ln(MeCN)_2^+$ (Ln=Y, Lu; Table 1). It is noted that the slightly larger Gd (1.107 Å vs. 1.075 Å for Y, 9-coordinate)[25] is known to coordinate 3 MeCN in the solid state.[26] When 2 equiv. of MeCN was introduced to complexes **1** and **2**, a small chemical shift (3.32 and 3.48 ppm, respectively) was observed that suggested no displacement (Figure S23). When 10 equiv. are added to complex **1**, the N_2H_4 resonance moves upfield to an intermediate value of 3.19 ppm. A NOESY evaluation indicates N_2H_4 is still bound (Figure S24). Complex **2** behaves in a similar fashion (Figure S25).

There are few examples in the literature of soft ligands, such as PMe_3, coordinating preferentially to lanthanide complexes. When P does coordinate, it generally requires no competition from harder atoms.[27,28] Our observed upfield shift (Figures S26 and S28) in the N_2H_4 resonance implied some displacement, but the lack of a ^{31}P NMR shift from unbound PMe_3 (Figures S27 and S29) suggests some interaction with N_2H_4 as the source of the change. These experimental observations are consistent with our predictions.

Lastly, our model predicts THF does not have sufficient coordinative strength to displace N_2H_4. This is confirmed by the literature synthesis of $(C_5Me_5)_2Sm(N_2H_4)(THF)BPh_4$ in THF solution as well as our own synthesis of the larger/smaller analogues, complexes **1**–**3**.

Conclusion

With our long-range goal of catalytically producing N_2H_4 in mind, we have explored how simple solvents may displace N_2H_4 from lanthanide complexes. Our modelling suggests strong sigma donors are required, namely Me_3PO, DMSO, and DMF. Experimentally we confirmed the qualitative trend that was predicted, although the absolute Δ_rG values seem to be systematically shifted in favor of the hydrazine displacement (disparity between the prediction and experiment seen in DMF and DMSO with complexes **2** and **3**, and DMAP with complex **1**). In particular, ^1H nuclear magnetic resonance shifts confirm our predictions for the largest lanthanide (lanthanum), likely because the least Lewis acid metal center yields weaker bonding interactions. Our continued work developing a catalytic cycle will be communicated forthwith.

Experimental Section

General synthesis of $[Cp^*_2Ln(THF)(N_2H_4)]BPh_4$

A 20–25 mM solution of $Cp^*_2LnBPh_4$ (Ln=La, Y, Lu) in THF was added to a vial containing N_2H_4 (1 equiv.). The solution was stirred for 5 min, filtered, and crystallized by vapor diffusion of pentane into THF at −30 °C, giving the product as colorless crystals.

$[Cp^*_2La(THF)(N_2H_4)]BPh_4$ (1): This complex was prepared as described above (0.105 g, 0.12 mmol, 84%). ^1H NMR (THF-d_8, 25 °C, 499.9 MHz): $\delta = 7.34$ (t, 8H, $J = 5$ Hz, *o*-BPh_4), 6.94 (t, 8H $J = 10$ Hz, *m*-BPh_4), 6.80 (t, 4H, $J = 10$ Hz, *p*-BPh_4), 3.52 (broad s, 4H, N_2H_4), 1.86 ppm (s, 30H, Cp*). $^{13}C\{^1H\}$ NMR (THF-d_8, 25 °C, 125 MHz): $\delta =$ 165.2 (q, $J = 50$ Hz, BPh_4), 137.3, 126.3 (q, $J = 4$ Hz, BPh_4), 122.6, 119.1, 11.1 ppm. IR: 3339 (w, N–H), 3269 (m, N–H), 3250 (m, N–H), 3054 (w), 2975 (m), 2909 (m), 2862 (m), 1590 (m), 1488 (m), 1422 (m), 1378 (w), 1277 (w), 1135 (m), 1007 (m), 921 (m), 870 (m), 748

(s), 709 (s), 611 cm^{-1} (s). Anal Calc'd C: 69.23 H: 7.50 N: 3.36. Found C: 68.94 H: 7.41 N: 3.45

$[Cp^*_2Y(THF)(N_2H_4)]BPh_4$ (2): This complex was prepared as described above (0.083 g, 0.102 mmol, 80%). ^1H NMR (THF-d_8, 25 °C, 499.9 MHz): $\delta = 7.34$ (t, 8H, $J = 5$ Hz, *o*-BPh_4), 6.94 (t, 8H $J = 10$ Hz, *m*-BPh_4), 6.79 (t, 4H, $J = 10$ Hz, *p*-BPh_4), 3.58 (s, 4H, N_2H_4), 1.83 ppm (s, 30H, Cp*). $^{13}C\{^1H\}$ NMR (THF-d_8, 25 °C, 125 MHz): $\delta = 165.3$ (q, $J = 50$ Hz, BPh_4), 137.4, 126.2 (q, $J = 4$ Hz, BPh_4), 122.4, 117.8, 11.4 ppm. IR: 3338 (w, N–H), 3286 (m, N–H), 3247 (m, N–H), 3059 (w), 3004 (w), 2905 (m), 2862 (m), 1588 (s), 1482 (m), 1437 (s), 1273 (w), 1187 (w), 1141 (m), 1022 (s), 927 (m), 875 (s), 852 (m), 751 (s), 718 (s), 609 (s), 458 cm^{-1} (s). Anal Cal'd C: 73.65 H: 7.98 N: 3.58. Found C: 73.64 H: 8.56 N: 3.64

$[Cp^*_2Lu(THF)(N_2H_4)]BPh_4$ (3): This complex was prepared as described above (0.015 g, 0.023 mmol, 70%). ^1H NMR (THF-d_8, 25 °C, 499.9 MHz): $\delta = 7.33$ (t, 8H, $J = 5$ Hz, *o*-BPh_4), 6.93 (t, 8H $J = 10$ Hz, *m*-BPh_4), 6.79 (t, 4H, $J = 10$ Hz, *p*-BPh_4), 3.60 (s, 4H, N_2H_4), 1.83 ppm (s, 30H, Cp*). $^{13}C\{^1H\}$ NMR (THF-d_8, 25 °C, 125 MHz): $\delta = 164.2$ (q, $J = 50$ Hz, BPh_4), 136.1, (q, $J = 4$ Hz, BPh_4), 125.1, 121.8, 114.9, 10.1 ppm. IR: 3328 (m, N–H), 3280 (m, N–H), 3239 (m, N–H), 3058 (w), 3037 (w), 2986 (m), 2913 (m), 2861 (m), 1627 (m), 2595 (s), 1481 (m), 1440 (w), 1430 (w), 1388 (m), 1243 (w), 1139 (m), 1025 (s), 921 (w), 859 (w). 755 (s), 703 (s), 610 cm^{-1} (m). Anal Calc'd C 66.36 H: 7.19 N: 3.22. Found C: 65.97 H: 7.12 N: 3.12

Sample procedure for competition studies

To an NMR tube containing $[Cp^*_2La(THF)(N_2H_4)]BPh_4$) in THF-$d_8$ (0.008 g, 0.01 mmol, 0.5 mL) was added a 5% by mass stock solution of DMSO in C_6D_6 (0.030 g, 0.021 mmol, 2 equiv.). The NMR tube was capped, shaken, and immediately taken to collect an NMR spectrum.

Computational details

PBE,[29] PBE0,[30,31] and B3LYP[32,33] functionals were compared regarding the evaluation of the Gibbs reaction energy (Table S7). Considering their qualitative agreement, B3LYP functional was used for further calculations. Grimme's D3 dispersion correction[34] was used in all DFT calculations. Conformational sampling of the complexes was performed using the Crest[35] program together with GFN2-xTB.[36] Structures were preoptimized on B3LYP/def2-SVP[37] level and further reoptimized together with frequency calculation on B3LYP/def2-TZVP level. MWB[38–40] pseudopotentials and corresponding basis sets were used for the metal centers. Solvation energy was obtained from single-point calculations with inclusion of the implicit solvent (THF, $\varepsilon = 7.4257$). Gaussian 16,[41] Revision C.01 software was used for the DFT calculations. Population and bonding analysis was performed on the local minima structures using the NBO 7.0 software.[42]

Acknowledgements

A.J. was sponsored by Fulbright-Masaryk scholarship during this work. We would like to thank the Los Alamos National Laboratory's Laboratory Directed Research and Development for funding of this work.

Conflict of Interest

The authors declare no conflict of interest.

Data Availability Statement

The data that support the findings of this study are available in the supplementary material of this article.

Keywords: coordination · energy storage · hydrazine · inorganic chemistry · lanthanide

[1] "USDOE Energy Storage Grand Challenge," can be found under https://www.energy.gov/energy-storage-grand-challenge/energy-storage-grand-challenge, **2020**.
[2] Y. Preger, L. Torres-castro, J. Mcdowall. "Lithium-ion Batteries" in *2020 USDOE Energy Storage Handbook*, https://www.sandia.gov/ess-ssl/eshb/.
[3] A. J. Headley, S. Schoenung, in *2020 USDOE Energy Storage Handb.*, **n.d.**, p. https://www.sandia.gov/ess-ssl/eshb/.
[4] A. Serov, C. Kwak, *Appl. Catal. B* **2010**, *98*, 1–9.
[5] L. Tamašauskaitė-Tamašiūnaitė, D. Šimkūnaitė, A. Nacys, A. Balčiūnaitė, A. Zabielaitė, E. Norkus, in *Direct Liq. Fuel Cells Fundam. Adv. Futur.* **2021**, pp. 233–248.
[6] E. W. Schmidt, *Hydrazine and its Derivatives: Preparation, Properties, Applications*, Wiley-Interscience, New York, **2001**.
[7] S. Kim, F. Loose, P. J. Chirik, *Chem. Rev.* **2020**, *120*, 5637–5681.
[8] A. E. Shilov, A. K. Shilova, E. F. Kvashina, T. A. Vorontsova, *J. Chem. Soc. D., Chem. Comm.* **1971**, 1590–1591.
[9] J. M. Manriquez, J. E. Bercaw, *J. Am. Chem. Soc.* **1974**, *96*, 6229–6230.
[10] T. A. George, D. J. Rose, Y. Chang, Q. Chen, J. Zubieta, *Inorg. Chem.* **1995**, *34*, 1295–1298.
[11] N. P. Mankad, M. T. Whited, J. C. Peters, *Angew. Chem. Int. Ed.* **2007**, *46*, 5768–5771; *Angew. Chem.* **2007**, *119*, 5870–5873.
[12] P. J. Hill, L. R. Doyle, A. D. Crawford, W. K. Myers, A. E. Ashley, *J. Am. Chem. Soc.* **2016**, *138*, 13521–13524.
[13] M. T. Mock, S. Chen, M. O'Hagan, R. Rousseau, W. G. Dougherty, W. S. Kassel, R. M. Bullock, *J. Am. Chem. Soc.* **2013**, *135*, 11493–6.
[14] L. D. Field, H. L. Li, P. M. Abeysinghe, M. Bhadbhade, S. J. Dalgarno, R. D. McIntosh, *Inorg. Chem.* **2019**, *58*, 1929–1934.
[15] P. Saha, S. Amanullah, A. Dey, *J. Am. Chem. Soc.* **2020**, *142*, 17312–17317.
[16] B. M. Lindley, A. M. Appel, K. Krogh-Jespersen, J. M. Mayer, A. J. M. Miller, *ACS Energy Lett.* **2016**, *1*, 698–704.
[17] R. Borup, J. Meyers, B. Pivovar, Y. S. Kim, R. Mukundan, N. Garland, D. Myers, M. Wilson, F. Garzon, D. Wood, P. Zelenay, K. More, K. Stroh, T. Zawodzinski, J. Boncella, J. E. McGrath, M. Inaba, K. Miyatake, M. Hori, K. Ota, Z. Ogumi, S. Miyata, A. Nishikata, Z. Siroma, Y. Uchimoto, K. Yasuda, K.-I. Kimijima, N. Iwashita, *Chem. Rev.* **2007**, *107*, 3904–3951.
[18] W. J. Evans, G. Kociok-kohn, J. W. Ziller, *Angew. Chem. Int. Ed.* **1992**, *31*, 1081–1082; *Angew. Chem.* **1992**, *104*, 1114–1115.
[19] W. J. Evans, G. Kociok-kohn, V. S. Leong, J. W. Ziller, *Inorg. Chem.* **1992**, *31*, 3592–3600.
[20] M. Fang, J. E. Bates, S. E. Lorenz, D. S. Lee, D. B. Rego, J. W. Ziller, F. Furche, W. J. Evans, *Inorg. Chem.* **2011**, *50*, 1459–1469.
[21] M. Fang, D. S. Lee, J. W. Ziller, R. J. Doedens, E. Bates, F. Furche, W. J. Evans, *J. Am. Chem. Soc.* **2011**, *133*, 3784–3787.
[22] Z. J. Lv, Z. Huang, W. X. Zhang, Z. Xi, *J. Am. Chem. Soc.* **2019**, *141*, 8773–8777.
[23] Structures JUFZUA and KOCDOX in the CSD.
[24] W. J. Evans, C. A. Seibel, J. W. Ziller, *J. Am. Chem. Soc.* **1998**, *120*, 6745–6752.
[25] R. D. Shannon, *Acta Crystallogr.* **1976**, *A32*, 751.
[26] J. F. Corbey, D. H. Woen, J. W. Ziller, W. J. Evans, *Polyhedron* **2016**, *103*, 44–50.
[27] T. D. Tilley, R. A. Andersen, A. Zalkin, *Inorg. Chem.* **1983**, *22*, 856–859.
[28] D. J. Schwartz, R. A. Andersen, *Organometallics* **1995**, *14*, 4308–4318.
[29] J. P. Perdew, K. Burke, M. Ernzerhof, *Phys. Rev. Lett.* **1996**, *77*, 3865–3868.
[30] C. Adamo, V. Barone, *J. Chem. Phys.* **1999**, *110*, 6158–6170.

[31] M. Ernzerhof, G. E. Scuseria, *J. Chem. Phys.* **1999**, *110*, 5029.
[32] A. D. Beck, *J. Chem. Phys.* **1993**, *98*, 5648–5656.
[33] C. Lee, C. Sosa, *J. Chem. Phys.* **1994**, *100*, 9018–9024.
[34] S. Grimme, J. Antony, S. Ehrlich, H. Krieg, *J. Chem. Phys.* **2010**, *132*, 154104.
[35] P. Pracht, F. Bohle, S. Grimme, *Phys. Chem. Chem. Phys.* **2020**, *22*, 7169–7192.
[36] C. Bannwarth, S. Ehlert, S. Grimme, *J. Chem. Theory Comput.* **2019**, *15*, 1652–1671.
[37] F. Weigend, R. Ahlrichs, *Phys. Chem. Chem. Phys.* **2005**, *7*, 3297–3305.
[38] D. Andrae, U. Häußermann, M. Dolg, H. Stoll, H. Preuß, *Theor. Chim. Acta* **1990**, *77*, 123–141.
[39] X. Cao, M. Dolg, *J. Chem. Phys.* **2001**, *115*, 7348–7355.
[40] M. Dolg, H. Stoll, H. Preuss, *Theor. Chim. Acta* **1993**, *85*, 441–450.
[41] M. J. Frisch, G. W. Trucks, H. B. Schlegel, G. E. Scuseria, M. A. Robb, J. R. Cheeseman, G. Scalmani, V. Barone, G. A. Petersson, H. Nakatsuji, X. Li, M. Caricato, A. V. Marenich, J. Bloino, B. G. Janesko, R. Gomperts, B. Mennucci, H. P. Hratchian, J. V. Ortiz, A. F. Izmaylov, J. L. Sonnenberg, D. Williams-Young, F. Ding, F. Lipparini, F. Egidi, J. Goings, B. Peng, A. Petrone, T. Henderson, D. Ranasinghe, V. G. Zakrzewski, J. Gao, N. Rega, G. Zheng, W. Liang, M. Hada, M. Ehara, K. Toyota, R. Fukuda, J. Hasegawa, M. Ishida, T. Nakajima, Y. Honda, O. Kitao, H. Nakai, T. Vreven, K. Throssell, J A. Montgomery, J. E. Peralta, Jr., F. Ogliaro, M. J. Bearpark, J. J. Heyd, E. N. Brothers, K. N. Kudin, V. N. Staroverov, T. A. Keith, R. Kobayashi, J. Normand, K. Raghavachari, A. P. Rendell, J. C. Burant, S. S. Iyengar, J. Tomasi, M. Cossi, J. M. Millam, M. Klene, C. Adamo, R. Cammi, J. W. Ochterski, R. L. Martin, K. Morokuma, O. Farkas, J. B. Foresman, D. J. Fox, *Gaussian 16 (Revision B.01)*, Gaussian, Inc., Wallingford CT, **2016**.
[42] E. D. Glendening, J. K. Badenhoop, A. E. Reed, J. E. Carpenter, J. A. Bohmann, C. M. Morales, P. Karafiloglou, C. R. Landis, F. Weinhold, *NBO 7.0*, Theoretical Chemisty Institute, **2018**.

Manuscript received: April 29, 2022
Revised manuscript received: July 18, 2022
Accepted manuscript online: July 21, 2022
Version of record online: August 9, 2022

